

This discussion paper is/has been under review for the journal Atmospheric Chemistry and Physics (ACP). Please refer to the corresponding final paper in ACP if available.

Assessing modelled spatial distributions of ice water path using satellite data

S. Eliasson¹, S. A. Buehler¹, M. Milz¹, P. Eriksson², and V. O. John³

¹Department of Space Science, Luleå Univ. of Technology, Kiruna, Sweden

²Department of Radio and Space Science, Chalmers Univ. of Technology, Göteborg, Sweden

³Met Office Hadley Centre, Exeter, UK

Received: 8 March 2010 – Accepted: 23 April 2010 – Published: 10 May 2010

Correspondence to: S. Eliasson (s.eliasson@ltu.se)

Published by Copernicus Publications on behalf of the European Geosciences Union.

IWP spatial distribution comparison

S. Eliasson et al.

Title Page

Abstract

Introduction

Conclusions

References

Tables

Figures

⏪

⏩

◀

▶

Back

Close

Full Screen / Esc

Printer-friendly Version

Interactive Discussion



Abstract

The climate models used in the IPCC AR4 show large differences in monthly mean cloud ice. The most valuable source of information that can be used to potentially constrain the models is global satellite data. For this, the data sets must be long enough to capture the inter-annual variability of Ice Water Path (IWP). PATMOS-x was used together with ISCCP for the annual cycle evaluation in Fig. 7, while ECHAM-5 was used for the correlation with other models in Table 3. A clear distinction between ice categories in satellite retrievals, as desired from a model point of view, is currently impossible. However, long-term satellite data sets may still be used to indicate the climatology of IWP spatial distribution. We evaluated satellite data sets from CloudSat, PATMOS-x, ISCCP, MODIS and MSPPS in terms of monthly mean IWP, to determine which data sets can be used to evaluate the climate models. IWP data from CloudSat cloud profiling radar provides the most advanced data set on clouds. As CloudSat data are too short to evaluate the model data directly, it was mainly used here to evaluate IWP from the other satellite data sets. ISCCP and MSPPS were shown to have comparatively low IWP values. ISCCP shows particularly low values in the tropics, while MSPPS has particularly low values outside the tropics. MODIS and PATMOS-x were in closest agreement with CloudSat in terms of magnitude and spatial distribution, with MODIS being the best of the two. As PATMOS-x extends over more than 25 years and is in fairly close agreement with CloudSat, it was chosen as the reference data set for the model evaluation. In general there are large discrepancies between the individual climate models, and all of the models show problems in reproducing the observed spatial distribution of cloud-ice. Comparisons consistently showed that ECHAM-5 is the GCM from IPCC AR4 closest to satellite observations.

IWP spatial distribution comparison

S. Eliasson et al.

Title Page

Abstract

Introduction

Conclusions

References

Tables

Figures



Back

Close

Full Screen / Esc

Printer-friendly Version

Interactive Discussion



1 Introduction

Ice clouds are an important part of the earth's climate system. Knowledge of the distribution and properties of ice clouds is central to understanding the atmospheric water budget, as their distribution strongly affects precipitation and the water cycle. Ice clouds also have a strong effect on the radiation budget of the atmosphere. They cool the atmosphere by reflecting incoming solar radiation, but also heat the atmosphere by absorbing and re-emitting outgoing terrestrial radiation. The magnitude of both processes, hence the net sum radiative impact of ice clouds, depends on macro-physical properties such as cloud top temperature, ice particle density, and vertical and horizontal extent, and on micro-physical properties such as ice crystal shape (Ramanathan et al., 1989). One important ice cloud quantity is the column integral of the cloud Ice Water Content (IWC) through the depth of the atmosphere. This quantity is called Ice Water Path (IWP) and commonly has the units g/m^2 .

There are large differences in IWP between climate models (John and Soden, 2006). The lack of adequate and abundant IWP measurements is the main problem in constraining climate models. In-situ data are important for validation, but they are few and far apart. Satellite IWP data, on the other hand, are global and continuous. However, the use of satellite data for model validation is also riddled with difficulties. This is largely due to the definition of IWP itself. Models make a clear distinction between precipitating-ice and cloud-ice, whereas observed IWP will contain a mixture of both. This must be taken into account in comparison studies such as this one. Despite these shortcomings, satellite data remain the most valuable source of information. There are many satellite data sets available that provide IWP, some with a temporal coverage of up to 25 years. However, satellite retrievals of IWP and other key properties related to ice clouds are still inadequate (e.g., Eriksson et al., 2008). Their accuracy is limited by assumptions that must be made in the retrieval, errors in a priori information, and instrument sensitivities. Different satellite data sets of IWP are derived using different retrieval techniques covering spectral bands ranging from microwave to visible using

IWP spatial distribution comparison

S. Eliasson et al.

Title Page

Abstract

Introduction

Conclusions

References

Tables

Figures



Back

Close

Full Screen / Esc

Printer-friendly Version

Interactive Discussion



passive or active sensors, each with inherent strengths and weaknesses. As a consequence of this, the different satellite data sets have a wide range of IWP values and distributions. The accuracy of IWP satellite retrievals has lately improved significantly through the introduction of data from CloudSat, which therefore is a key data set in this article.

This article provides a comprehensive comparison of satellite data sets that provide IWP information that can potentially be used to constrain model IWP output. In particular, we anchored monthly mean IWP of long term satellite data sets to CloudSat. CloudSat retrieval accuracies have been previously quantified using in situ data from several campaigns in Heymsfield et al. (2008). We also evaluated the performance of various climate models in terms of distribution of monthly mean IWP on climatic time scales. The climate models used in this study are included in the fourth assessment report (AR4) of the Intergovernmental Panel on Climate Change (Intergovernmental Panel on Climate Change, 2007). As described by Waliser et al. (2009), the models disagree significantly with regards to the magnitude and spatial distribution of IWP. The general lack of IWP measurements to validate against and the assumptions made about ice particle size, mass, and cross-sectional area, which directly influence particle fall velocities (Heymsfield and Iaquinta, 2000), are likely to play an important role. There are also large differences between the models in terms of absolute column water mass (Precipitable Water, Liquid Water Path and IWP) and statements made about the absolute differences in IWP should take this into account.

The aim of the article is to provide an overview on how the satellite data sets compare to each other, using monthly mean IWP measurements, and what the climatic global distributions of IWP are. These results are further used to evaluate a sub-set of climate models in terms of magnitude and spatial distribution of IWP. Section 2 provides short descriptions of the chosen climate models and satellite data sets. Section 3 provides quantitative and qualitative results from the comparison study, and satellite data set comparisons and satellite-model comparisons are done in parallel throughout the results section. Section 4 contains the discussion and conclusion.

**IWP spatial
distribution
comparison**

S. Eliasson et al.

Title Page

Abstract

Introduction

Conclusions

References

Tables

Figures

◀

▶

◀

▶

Back

Close

Full Screen / Esc

Printer-friendly Version

Interactive Discussion



2 Description of data sets

2.1 General circulation models

All models in AR4 provide monthly cloud-ice averages with a temporal range of at least 100 years from 1900. For the remainder of the article, model “cloud-ice” will be simply be referred to as IWP. Table 1 shows the details of the AR4 models referred in this article. Table details include the short name further used in this article, the model resolution, the full name of the model, and the institute. They are presented in no particular order. Further descriptions of the climate models in AR4 can be found at http://www-pcmdi.llnl.gov/ipcc/model_documentation/ipcc_model_documentation.php.

We have chosen a group of 6 models that roughly represent the inter-model variability of IWP of all models in AR4. ECHAM is a high resolution model with comparatively low IWP values, CCSM has the highest resolution and the lowest IWP averages of all models, CSIRO has a relatively high horizontal resolution and relatively high IWP averages, GISS has the coarsest resolution and has very high IWP averages, INM is a low resolution model with very low IWP values in general, and UKMO has a relatively high resolution and shows remarkably low IWP values in the tropics compared to outside the tropics.

2.1.1 Common model features

In general, GCMs generate ice clouds through the convergence of moist air masses leading to condensation by large scale dynamics. This is added to the existing cloudiness in the grid box previously determined either diagnostically by relative humidity or prognostically as cloudiness from an earlier time step. Moist convection also adds cloud-ice to existing ice cloud. When comparing climate model output to satellite data, it is important to recognise that the representation of IWP is only comparable to satellite observations to a certain extent. Climate models distinguish between precipitating ice, such as snow and graupel, and cloud-ice, which remains suspended aloft. The

IWP spatial distribution comparison

S. Eliasson et al.

Title Page

Abstract

Introduction

Conclusions

References

Tables

Figures

◀

▶

◀

▶

Back

Close

Full Screen / Esc

Printer-friendly Version

Interactive Discussion



precipitated ice is removed at each time step and it either sublimates as it falls out or reaches the ground as precipitation. Only the cloud-ice remaining from these processes is saved as a diagnostic variable. This is the parameter that is saved in the AR4 archive. Waliser et al. (2009) suggest models may have global cloud-ice fractions in the order of 0.1 to 0.3 of the total modelled ice particle mass. They further argue that satellite retrievals of ice clouds do not make a distinction between the ice particles as the models do and this must also be taken into account in all model-satellite comparisons.

2.2 Satellite IWP data sets

IWP is retrieved over a wide radiative spectrum, ranging from microwave to visible wavelengths using active or passive instruments. We have sampled data sets with retrievals throughout this range. The satellite data sets used in this survey are presented in no particular order below.

2.2.1 CloudSat

CloudSat data are provided by Colorado State University and NASA Jet Propulsion Laboratory. CloudSat is in the A-train, which is a constellation of satellites flying in close formation enabling maximum collocations between these satellites (Stephens et al., 2002). To date, it provides the most advanced satellite data set on clouds. In contrast to the other satellite data sets in the survey, which are based on passive remote sensing techniques, CloudSat is based on an active sensor. The CloudSat satellite has a 94 GHz, 0.16° off-nadir looking Cloud Profiling Radar. It has a high vertical resolution of 500 m, enabling the retrieval of cloud vertical structures and has a small horizontal footprint of approximately 1.5 km. Because CloudSat does not scan across-track, the small footprint size leads to poor horizontal coverage which results in data sampling artifacts when averaging the data. We have addressed this issue by binning CloudSat data onto a coarse grid of 5°. The IWP product used in this study (RO_ice_water_path)

IWP spatial distribution comparison

S. Eliasson et al.

Title Page

Abstract

Introduction

Conclusions

References

Tables

Figures



Back

Close

Full Screen / Esc

Printer-friendly Version

Interactive Discussion



is retrieved from radar only data and the model temperature data from the ECMWF model (the CloudSat ECMWF AUX product). The algorithms used for this product is described in Austin et al. (2009). On-line descriptions of CloudSat products are also available at the website: <http://www.cloudsat.cira.colostate.edu/dataSpecs.php>.

5 A major source of uncertainty in CloudSat, comes from clouds that may or may not be ice clouds. CloudSat retrievals use a linear liquid to ice ratio as a function of temperature, where all clouds warmer than 273 K are liquid clouds and all clouds colder than 243 K are ice clouds. For ice clouds, results from Heymsfield et al. (2008) indicate that CloudSat IWC retrievals are within $\pm 40\%$ of in-situ measurements (Austin et al., 2009; Waliser et al., 2009). Yet, this error estimate is conservative for IWP, as averaging the IWC errors in a column should lead to a reduced error. On the other hand the sample from which the 40% error estimate is determined is small, and the study used simulated satellite data rather than real data, so the true error may even be larger than 40%. In the absence of other information, we assume that 40% is a realistic error estimate for CloudSat IWP. We have used all available CloudSat IWP data covering the temporal range of July 2006 to August 2009.

2.2.2 ISCCP

IWP data are provided by the International Satellite Cloud Climatology Project (IS-CCP). The D2 data set, which contains monthly averages, is based on one Infrared (IR) channel around $11 \mu\text{m}$ and one visible channel around $0.6 \mu\text{m}$. This is the only data set that uses data from geostationary satellites. Radiance data are collected from five geostationary satellites and two polar orbiting satellites, although data from polar-orbiting satellites are complementary and used mainly at high latitudes. The geostationary satellites are a combination of METEOSAT satellites from EUMETSAT, GOES satellites from the United States and GMS satellites from Japan. The polar orbiting satellites are from the National Oceanic and Atmospheric Administration (NOAA) series from the United States (Rossow and Schiffer, 1991). As ISCCP is mainly based on geostationary satellites, it is best at tropical latitudes. However, until 1997 there was

IWP spatial distribution comparison

S. Eliasson et al.

Title Page

Abstract

Introduction

Conclusions

References

Tables

Figures

◀

▶

◀

▶

Back

Close

Full Screen / Esc

Printer-friendly Version

Interactive Discussion



IWP spatial distribution comparison

S. Eliasson et al.

Title Page

Abstract

Introduction

Conclusions

References

Tables

Figures

◀

▶

◀

▶

Back

Close

Full Screen / Esc

Printer-friendly Version

Interactive Discussion



a systematic gap in data coverage over the Indian Ocean and this effect can be seen in the merged data prior to this date. Data from ISCCP are gridded using an equal area grid described in Rossow and Garder (1984), and have a horizontal resolution of $2.5 \times 2.5^\circ$ at the equator. ISCCP does not provide IWP directly. Instead, Water Path monthly means are provided for 15 distinct cloud types, classified according to their cloud top temperature, cloud top pressure, and cloud optical thickness. According to these classifications, an ice cloud is a cloud that has a cloud top temperature colder than 260 K or has a cloud top pressure less than 440 hPa. In much the same approach used in Storelvmo et al. (2008), IWP is calculated from the sum of Water Path values from all cloud types classified as ice clouds. The difference in approaches lies in that Storelvmo et al. (2008) partly reclassify ice clouds in the tropics into liquid clouds, whereas we have decided not to reclassify any clouds. Refer to Rossow and Schiffer (1991) or the web page: <http://isccp.giss.nasa.gov/docs/D-toc.html> for a detailed description of the algorithms used in the ISCCP retrievals. This data set extends from July 1983 to June 2008.

2.2.3 PATMOS-x

The Pathfinder Atmospheres- Extended (PATMOS-x) data set, from the Cooperative Institute for Meteorological Satellite Studies, provides an IWP data product based on visible, near infrared, and infrared radiances. An algorithm to derive IWP is applied to AVHRR radiance data to detect clouds and perform the retrieval. The AVHRR instrument is flown on the NOAA Polar-orbiting Operational Environmental Satellites (POES). The PATMOS-x data used in this survey are monthly mean IWP, gridded on a similar grid as ISCCP, but with a resolution of 0.5° at the equator. Data from PATMOS-x span the longest time period in the survey (January 1982 to April 2008). Information about the data set including how to obtain it is available at the web site: <http://cimss.ssec.wisc.edu/patmosx/>.

2.2.4 MODIS

IWP data are also available from the NASA Moderate Resolution Imaging Spectroradiometer (MODIS). As with PATMOS-x, IWP is retrieved from visible, near infrared, and infrared channels, yet at a higher spectral resolution than data from AVHRR. The MODIS instrument is down-looking with a total of 36 spectral channels, and 13 of them are used for retrieving cloud properties. The MODIS instrument is on board the Earth Observing Satellites, Aqua and Terra, where Aqua is located in the A-train (Stephens et al., 2002). All MODIS data are screened using a cloud mask described in Ackerman et al. (2008), and details on the retrieval are described in King et al. (1997). The MODIS data used in this survey are the level 3 monthly cloud product (MYD08_03, collection version 5), column integrated IWP, with a 1° gridded spatial resolution. We have chosen to solely focus on data from Aqua as its data are collocated with CloudSat. The MODIS data used in this survey extends from July 2002 to December 2008.

2.2.5 MSPPS

Satellite IWP data from passive microwave sensors are also used in this survey and are provided by the Microwave Surface and Precipitation Products System (MSPPS) from the National Environmental Satellite, Data and Information Service. The MSPPS IWP product is retrieved using the AMSU-B sensor which has 5 channels ranging from 89 GHz to 183.3 GHz. AMSU is flown on the NOAA POES satellites. For further details regarding the AMSU-B instrument, refer to Atkinson (2001). For a description of the MSPPS IWP product and others derived from AMSU refer to Ferraro et al. (2005). As the satellite NOAA-18 has the largest number of collocations with CloudSat, we have chosen to focus on MSPPS data from NOAA-18 only. AMSU-B was replaced by the Microwave Humidity Sounder (MHS), which is very similar in design to its predecessor on NOAA18. MSPPS data used in this survey extend from October 2005 to December 2009.

IWP spatial distribution comparison

S. Eliasson et al.

Title Page

Abstract

Introduction

Conclusions

References

Tables

Figures



Back

Close

Full Screen / Esc

Printer-friendly Version

Interactive Discussion



2.2.6 Satellite data set summary

Refer to Table 2 for an overview of the data sets used in this survey. The table provides the short name, the instruments used in the retrievals, the satellite platforms and the institutions associated with these products. Comparing satellite data sets of retrieved IWP is not straight forward. One major contributing factor to this is the uncertainty in determining the cloud top and cloud base from retrievals (Wu et al., 2009). This uncertainty is inevitable as cloud-ice signals are generally stronger for high frequencies (VIS, IR) than for low frequencies (passive microwave, radar). This is partly due to the wavelength relative to the size of the cloud particles, influencing the particles scattering properties. Retrievals of IWP based on microwave frequencies such as MSPPS and CloudSat, have difficulties detecting thin Cirrus clouds, but can retrieve cloud information deeper into thick ice clouds than retrievals based on IR or VIS instruments. On the other hand, retrievals such as used in ISCCP, PATMOS-x and MODIS, detect more thin clouds. In truth, all satellite IWP retrievals portray only part of the true IWP column (Waliser et al., 2009). As a consequence, the distribution and, especially, the magnitude of IWP is expected to vary between data sets and this must be taken into account when comparing data sets. As CloudSat IWP has been validated, CloudSat will be the main reference data set. However, CloudSat is not suitable for climate model comparisons of monthly mean IWP. CloudSat spans a short time period of a mere 3 years and also has poor horizontal coverage, as mentioned earlier. The short time span is especially important, in that models are not expected to model individual years but rather climatic temporal ranges. Indeed, most of the time period in which CloudSat has been operational, La Niña-type conditions have been dominant. Although the models capture inter-annual variations and may predict the correct variability, the timing of these events will not coincide with the real world variation. Furthermore, the poor horizontal coverage of CloudSat introduces problems of data sampling leading to aliasing effects, which hampers any comparison studies to gridded data. Therefore we need to use satellite data sets with longer temporal ranges and a higher spatial coverage. As both

IWP spatial distribution comparison

S. Eliasson et al.

Title Page

Abstract

Introduction

Conclusions

References

Tables

Figures



Back

Close

Full Screen / Esc

Printer-friendly Version

Interactive Discussion



PATMOS-x and ISCCP have long temporal ranges, they capture the inter-annual variations of IWP, and can therefore be used to validate the models. PATMOS-x, MODIS and MSPPS have high spatial coverage useful for spatial distribution comparisons to models.

3 Observations and results

3.1 Zonal averages

Figure 1 depicts the zonal mean IWP for the satellite data sets, compared on a common period (July 2006 to April 2008). An uncertainty interval, indicated as the grey shaded area, is included for reference and is based on the uncertainty of CloudSat measurements (40%). Large differences between the satellite data sets are apparent. As mentioned in Sect. 2.2.6, these differences can be attributed to instrumental sensitivities and the retrievals used. MODIS is in best agreement with CloudSat, and is the only satellite data set that has zonal averages inside CloudSat's uncertainty interval at all latitudes. The IWP distribution of MODIS appears to agree best outside the tropics, as it has a sizable bias in the tropics, albeit within the CloudSat's uncertainty. PATMOS-x IWP distribution has a very large positive bias outside the tropics, but for tropical latitudes, it is close to the upper limit of the CloudSat uncertainty. While MODIS is in slightly better agreement with CloudSat than PATMOS-x in the tropics, their absolute bias is about the same size. ISCCP appears to have much lower IWP values in general, with particularly low values in the tropics, where convection dominates. We attribute this mostly to the difficulty in achieving accurate retrievals of optically thick clouds. MSPPS has the lowest zonal averages of IWP, probably because many clouds are completely undetected. In contrast to ISCCP, MSPPS has its largest IWP averages in tropical areas, whereas in mid-latitudes regions, which are dominated by less thick ice clouds, MSPPS has very low values. This can be explained as MSPPS retrievals are particularly sensitive to large ice particles associated with convective clouds. All

IWP spatial distribution comparison

S. Eliasson et al.

Title Page

Abstract

Introduction

Conclusions

References

Tables

Figures

◀

▶

◀

▶

Back

Close

Full Screen / Esc

Printer-friendly Version

Interactive Discussion



passive satellite data sets perform very poorly over snow covered regions (not shown), as a signal from the cold surface is often indecipherable from a signal from thick ice clouds, and therefore erroneously detected as clouds with high IWP values. For this reason all data outside the latitude range 60 S–60 N are not used.

5 Figure 2 shows the zonal mean IWP for the models using all available data. An uncertainty interval is also included here. However, for a fair comparison, CloudSat error was combined with the uncertainty associated with differing model fractions of cloud-ice mass to total column mass of ice particles. The fraction of cloud-ice is not disclosed by the models in AR4, but cloud-ice fractions of two models, were presented in Figs. 10 and 11 in Waliser et al. (2009). These models are, the NASA Goddard finite-volume Multi-scale Modeling Framework model (fvMMF hereafter) and the Weather Research and Forecasting (WRF) model using the Reduced Acceleration in the VERTICAL (RAVE) approach (RAVE hereafter). Through lack of options, these two models were chosen to represent the upper and lower limits of cloud-ice fractions of all GCMs. RAVE generally has a consistently higher cloud-ice fraction over all latitudes compared to fvMMF. Therefore, to estimate the upper limit of the uncertainty, we multiplied its zonal average cloud-ice fraction with the upper uncertainty boundary of CloudSat (see Fig. 1). In the same manner, the lower uncertainty limit was determined by multiplying the zonal average cloud-ice fraction of fvMMF with the lower boundary of CloudSat's uncertainty.

20 It is clear that there are large differences between observed and modelled IWP averages, but also between the models themselves. With the exception of GISS, CloudSat has IWP values between two to ten times higher than the climate models (compare Fig. 1 and Fig. 2). The relatively low modelled IWP values are mostly due to the distinctions made between modelled ice particles. Model IWP only represents cloud-ice and does not include precipitating snow and graupel, whereas IWP from CloudSat (and all other satellite data sets) represents all ice particles. However, set against the uncertainty range based on the aforementioned cloud-ice condition in conjunction with CloudSat's uncertainty interval, it seems that the models may overestimate cloud-ice around the mid-latitudes and slightly underestimate cloud-ice in the tropics. On the

IWP spatial distribution comparison

S. Eliasson et al.

[Title Page](#)[Abstract](#)[Introduction](#)[Conclusions](#)[References](#)[Tables](#)[Figures](#)[⏪](#)[⏩](#)[◀](#)[▶](#)[Back](#)[Close](#)[Full Screen / Esc](#)[Printer-friendly Version](#)[Interactive Discussion](#)

other hand, this statement is quite uncertain, as the actual cloud-ice fraction of the models is not provided.

Additional uncertainties in comparing satellite to model data were highlighted in Waliser et al. (2009). They explained the importance of diurnal sampling, i.e. pairing the model data to equivalent satellite overpasses, as satellite retrieved IWP may fluctuate in the order of $\pm 50\%$ from the mean value in the tropics. They also mentioned the need to take sensor and algorithm sensitivities into consideration when comparing satellite to model measurements, in that sensitivities have an upper and lower limit, while models do not. We have decided to neglect these effects, as this paper concerns the comparison of modelled monthly mean IWP, to several satellite data on a climatic time scale. Waliser et al. (2009) reported that even amongst some more sophisticated models, their zonal averages were in disagreement with satellite data, albeit in the vertical distribution of IWP (IWC). Figures 1 and 2 verify this, but much information is lost by averaging zonally. In zonal averaging, information on the longitudinal inhomogeneity of IWP distributions are lost. Therefore, in order to learn more about the differences in IWP between data sets, we also assess the spatial distribution of IWP. In this way we may understand if the differences are larger in some regions than others.

3.2 Spatial distribution of IWP

Figure 3 shows the spatial distribution of CloudSat IWP between 60N and 60S is shown on a 5° grid. CloudSat has particularly elevated IWP values around the Indonesian archipelago, a region often referred to as the Tropical Warm Pool (TWP), because of the very warm ocean in this region. This region has the highest IWP values globally. The Inter-Tropical Convergence Zone (ITCZ) is clearly visible along the equator of the Pacific and Atlantic Oceans. High values of IWP are observed over the TWP, ITCZ and mid-latitude storm tracks. As there is a very large spread in IWP values across all data sets, to facilitate a qualitative evaluation of the distributions, we first normalised the data. Despite the distribution of gridded IWP values being highly non-Gaussian, the magnitude of the mean and standard deviations of the data sets are somewhat linearly

IWP spatial distribution comparison

S. Eliasson et al.

Title Page

Abstract

Introduction

Conclusions

References

Tables

Figures

◀

▶

◀

▶

Back

Close

Full Screen / Esc

Printer-friendly Version

Interactive Discussion



related. For example, data sets with large mean values tend to have large standard deviations. Due to this, we chose to normalise IWP by subtracting the area weighted total mean IWP from the IWP distribution. By then dividing by the total standard deviation, normalised IWP can be expressed in terms of standard deviations about the mean:

$$\hat{X} = \frac{X - \bar{X}}{\sigma_x}$$

The normalised IWP is denoted \hat{X} , the original IWP is X , the total mean IWP is \bar{X} and the standard deviation of the gridded total IWP is σ_x . The latter two quantities are scalars.

Figure 4 shows the normalised spatial distribution of IWP for the satellite data sets on a common temporal range (July 2006 to April 2008). The top left panel is CloudSat data on a 1° grid and the top right figure is CloudSat data on a 5° grid. As demonstrated in the figure, retrieving spatial statistics from CloudSat data on a small grid is inappropriate. Due to the highly variable nature of IWP, data measurements are too sparse to attain a representative gridded monthly mean on a finer grid. Further spatial statistics of CloudSat are calculated on a 5° grid. Judging from the spatial distribution of MSPPS, it is obvious that its strength lies in detecting IWP of thick ice clouds, such as associated with deep convection. This may be due to MSPPS insensitivity to small ice particles and deep convective weather probably containing the highest fraction of large ice particles. This can be seen through relatively elevated values over tropical land masses where deep convection is also most common. Outside the tropics, many clouds are undetected as they are not as dense, resulting in low IWP averages. ISCCP shows low IWP values in general compared to CloudSat, PATMOS-x and MODIS, with particularly low IWP values in the convection dominated tropics. Waliser et al. (2009) argue that ISCCP IWP is expected to roughly apply to cloud-ice as it is insensitive to precipitation. The zonal average of the RAVE model may indicate that some models predict a larger fraction of cloud-ice at high-latitudes than the tropics (see Fig. 10e in Waliser et al., 2009). The observed spatial distribution of ISCCP data in Fig. 4 is consistent with that prediction. Figure 4 also supports our earlier analysis that in terms of

IWP spatial distribution comparison

S. Eliasson et al.

Title Page

Abstract

Introduction

Conclusions

References

Tables

Figures



Back

Close

Full Screen / Esc

Printer-friendly Version

Interactive Discussion



**IWP spatial
distribution
comparison**

S. Eliasson et al.

Title Page

Abstract

Introduction

Conclusions

References

Tables

Figures

◀

▶

◀

▶

Back

Close

Full Screen / Esc

Printer-friendly Version

Interactive Discussion



magnitude, PATMOS-x is close to the upper uncertainty limit of CloudSat in the tropics, with a somewhat larger positive bias within $\pm 60^\circ$ of the equator. The PATMOS-x IWP retrieval is strongly influenced by snow covered areas (not shown). Furthermore, Fig. 4 confirms that MODIS is in good agreement with CloudSat outside the tropics, but has a clear negative bias in the tropics. In general, as expected, the satellite data sets agree on the spatial distribution of key dynamical features such as the extent of the TWP and ITCZ, but do not show the same level of agreement at higher latitudes. As mentioned in Sect. 2.2, some differences in the magnitude and distribution of IWP between satellite data sets are expected. There is a large negative bias for cloud-ice outside the tropics in the MSPPS distribution, whereas IWP is relatively higher outside the tropics for data sets using IR/VIS techniques, such as PATMOS-x, ISCCP and MODIS.

Figure 5 shows the spatial distribution of normalised IWP for the selected climate models, averaged over all available years (approximately 100 years). The size and location of key dynamical features differs between the models. All models show elevated IWP averages around the oceanic westerlies of both hemispheres, although the magnitude of IWP varies considerably. The models also depict, to a varying extent, large regions of low IWP values in the tropical and subtropical Eastern Pacific and Indian Oceans. Notably, the ratio of magnitudes of IWP between tropical regions and temperate regions varies greatly from model to model. The most obvious inter-model differences lie in the tropics. The location of dynamical features in the tropics such as TWP, ITCZ and subsidence zones is corroborated by observations in Fig. 4. Figure 5 (and Table 3, introduced later) indicate that it is at tropical latitudes that the models are in greatest disagreement. Some models, (e.g. GISS and INM) show a large area of elevated IWP, misplaced well west of the TWP. In addition, some models (e.g. GISS) present a distinct dry zone along the equator deep into the TWP, also diminishing the ITCZ. There is a strong local maximum over Southern China in some models, whilst other models completely lack this feature. The GISS model has extremely elevated values (orders of magnitude higher than its total mean IWP) in this area. This feature is not corroborated by the distribution of IWP of any of our selected satellite data sets

(see Fig. 4). It is also clear that some models (e.g. UKMO) have low IWP values in the Tropics suggesting that IWP in convective clouds may not be included.

3.3 Monthly mean IWP

Modelled monthly mean IWP only very roughly represents the amount of ice in the atmosphere, where small scale processes such as convection and processes dependent on the diurnal cycle are parametrised. Figure 6 shows the histogram of CloudSat IWP measurements from the combined regions of equatorial continental convection in South America and Africa in March 2007. Intense convection in the region contributes to a mean IWP of 180 g/m^2 and a large variability of 743 g/m^2 . Despite high rainfall amounts in these regions, the ratio of cloudy pixels is only ca. 40%. The median IWP value of the cloudy pixels, defined as $\text{IWP} > 0$ for CloudSat measurements, is only 39 g/m^2 . By comparison, the global mean of all CloudSat IWP measurements for the same month (not shown) is 73 g/m^2 , and the median cloudy IWP value is 33 g/m^2 for the global IWP measurements. It is clear that the mean IWP is often very far from the IWP experienced at any given time. It is also clear from Fig. 6 that the distribution of IWP values is highly non-Gaussian, indicating that the use of Gaussian statistics, such as mean and standard deviation may not be best way to represent the monthly state of the atmosphere. Despite this, mean IWP is the common statistic used by models and satellite data sets when representing the data on a monthly basis. As results show, estimating the monthly cloud radiative forcing from monthly mean IWP is inappropriate, such as due to the non-linearity of the cloud radiative feedback (e.g., Atlas et al., 1995). This is especially valid in convective regions, where the mean and median cloud values differ the most.

3.4 Total statistics

Table 3 contains the area-weighted mean IWP of the selected satellite and climate model data sets for the total region (60 S–60 N) and the tropical region (30 S–30 N).

IWP spatial distribution comparison

S. Eliasson et al.

Title Page

Abstract

Introduction

Conclusions

References

Tables

Figures

◀

▶

◀

▶

Back

Close

Full Screen / Esc

Printer-friendly Version

Interactive Discussion



**IWP spatial
distribution
comparison**

S. Eliasson et al.

Title Page

Abstract

Introduction

Conclusions

References

Tables

Figures

◀

▶

◀

▶

Back

Close

Full Screen / Esc

Printer-friendly Version

Interactive Discussion



We have only used monthly mean values from 2007 for the satellite statistics, as this is the only full year where we have data from all data sets. As indicated, the satellite data sets are in better agreement, in terms of spatial and temporal correlation in the tropical region than in the total region. MODIS and PATMOS-x are in closest agreement with CloudSat and are within, or close to CloudSat's $\pm 40\%$ uncertainty interval in both regions. MODIS is in better agreement in the total region (which includes the tropics) than in the tropical region, whereas PATMOS-x tends to agree better with CloudSat within the tropical region. PATMOS-x deviates strongly from the other data sets at latitudes greater than 50° N/S (not shown). MSPPS has a large negative IWP bias in both regions, clearly indicating a general problem with its IWP retrieval. ISCCP has a large negative bias in general, tending towards a larger negative bias in the tropics. A more detailed regional analysis of IWP averages is further presented in Sect. 3.6.

Month averages based on model data from 1900–2000, were used for the model statistical comparison. Due to the long time series, the inter-annual variability is captured in the model statistics. Compared to the satellite data, the models, with the exception of GISS, clearly have much smaller IWP magnitudes, with averages ranging from 30–50% of the CloudSat average. As mentioned earlier, this is expected as model IWP pertains to the cloud-ice portion of the IWP column only. For this reason we have arbitrarily chosen ECHAM as a reference model for the models. In terms of spatial-monthly correlation, the models appear in better agreement with each other in the total region, whereas in the tropical region, the models deviate strongly from one another. The models, except for INM, also have much higher IWP averages in the total region than in the tropical region. UKMO exhibits nearly a factor 4 higher IWP values in the total region, whereas INM has the same average for both regions. ECHAM, CCSM and CSIRO are generally well correlated in both regions, but CCSM has much lower IWP values. GISS has a very large IWP magnitude across all latitudes and clearly exhibits problems modelling this quantity.

In summary, the satellite data sets are in better agreement in the tropics than outside the tropics, especially in terms of spatial distribution of IWP. The climate models, on the

other hand, appear to have the opposite relation.

3.5 IWP annual cycle

In this section, to check the model IWP variability compared to observations, we provide a qualitative evaluation of the large-scale annual cycle of IWP in the tropics (30 S–30 N). The annual cycle is measured here using the coefficient of variation (CV) (e.g., Mohapatra et al., 2007). CV is the variation of monthly mean IWP normalised by the mean of the monthly averages. A value is assigned to each grid box using:

$$CV = \frac{\sigma_I}{\bar{I}}$$

Where \bar{I} is the mean IWP of all months per grid box and σ_I is the standard deviation of the monthly means per grid box.

Figure 7 shows the annual cycle of observed and modelled IWP. PATMOS-x and ISCCP were chosen as observational data due to their long temporal ranges (25 and 24 years). Their long temporal ranges allow for the capture of the inter-annual variability, which is present in the models. In the observed data, the spatial distribution of CV indicates broad areas around the TWP, which on a relative scale have little variability. This indicates semi-persistent year round rainfall in this region. As expected, the yearly monsoonal activity gives rise to a large variability of monthly IWP near the Indian subcontinent, Northern Australia and Eastern Africa. Both PATMOS-x and ISCCP also indicate a region with a strong annual cycle in the Eastern Pacific. This feature is associated with an apparent “second ITCZ” that forms during March and April.

For the models, the annual cycle of IWP in CSIRO, ECHAM and INM closest resembles those seen in observations. Although, CSIRO and ECHAM have much smaller regions of low CV east and west of the TWP. CCSM underestimates the variability over India and has an area with large CV values west of Australia, a feature not seen in the observations or any other models. GISS completely lacks the area of low annual cycle associated with the TWP and its adjacent areas, indicating too large variability here.

IWP spatial distribution comparison

S. Eliasson et al.

Title Page

Abstract

Introduction

Conclusions

References

Tables

Figures

⏪

⏩

◀

▶

Back

Close

Full Screen / Esc

Printer-friendly Version

Interactive Discussion



The annual cycle in UKMO is very different from observations and other models. In general, the models poorly reflect the observed distribution of CV, i.e. the annual cycle. This indicates that important large scale seasonal processes in the tropics are poorly represented by the models in AR4.

3.6 Statistics by region

Waliser et al. (2009) compared the average global, tropical (30° S–30° N) and extra-tropical (>° N, S) IWP for both observational data sets and GCMs. They found these averages were approximately the same for each satellite data set. Whereas for the GCMs, they reported that extra-tropical averages were often more than a factor 2 larger than the tropical averages. We have chosen to go a step further and analyse the regional averages of satellite and model data in regions that, over all seasons, contain quasi-homogeneous atmospheric conditions. We have defined 4 large regions, each with a climate dominated by a large scale vertical motion of the atmosphere, either subsiding or rising.

We have selected two very large subsidence zones west of South America and west of South Africa, and these areas combined constitute the oceanic subsidence region (ocean_sub). Tropical continental South America and Africa together constitute the tropical continental convection region (trop_cont). The TWP and areas adjacent constitute the Tropical Oceanic Convection region (warm_pool). The areas of mid-latitude storms in the North Atlantic and North-West Pacific together constitute a region called westerlies. The boundaries of these regions are chosen based on the spatial distribution of IWP of all satellite data sets, and the largest possible regions with similar IWP distributions were selected. The extent of these regions are shown in Fig. 8.

The area-weighted mean and the regional fraction of IWP was calculated for satellite data sets and models for the chosen regions. The regional fraction in percent (IWP_{rel}) is defined:

$$IWP_{rel} = \frac{IWP_{reg}}{IWP_{tot}} \quad (1)$$

IWP spatial distribution comparison

S. Eliasson et al.

Title Page

Abstract

Introduction

Conclusions

References

Tables

Figures

◀

▶

◀

▶

Back

Close

Full Screen / Esc

Printer-friendly Version

Interactive Discussion



where IWP_{reg} is the mean IWP value for a given region and IWP_{tot} is mean IWP from the total region (60S – 60N) for each data set. This quantity was included for clarity, as the difference in the mean IWP between data sets is large. The aforementioned statistics are provided in Table 4 with IWP_{rel} given in brackets. The mean IWP in the total region has been included in the table as a reference (far right).

3.6.1 Regional observations

All satellite data sets, except for PATMOS-x, are in agreement in the oceanic subsidence regions, and their IWP fraction relative to the total mean lies between 4–8%. PATMOS-x has high IWP averages in these regions (3× larger than CloudSat). PATMOS-x can detect thinner ice clouds than CloudSat can, such as clouds induced from gravity waves or remnant outflow from distant convection, but this is not likely the cause of PATMOS-x's high relative values in these regions as MODIS, also based on similar spectral channels, does not show the same result. It is more likely that PATMOS-x has a problem here.

In the westerlies region, ISCCP has the highest relative fraction of the total average (1.9), PATMOS-x and MODIS have the same fraction (1.6), CloudSat (1.4) and MSPPS has the lowest fraction (0.4). This supports the notion that the cloud-ice fraction of the total IWP may be larger in this region. As mentioned earlier, ISCCP is mainly sensitive to cloud-ice and CloudSat is more sensitive to larger particles. MSPPS clearly has much too low IWP averages in this region.

As expected, the reverse is true for the maritime tropical convective region. MSPPS and CloudSat have the highest fractions (2.6 and 2.3) followed by PATMOS-x and MODIS (1.9 and 1.8), whilst ISCCP has the lowest fraction (1.5). This supports the notion that clouds may have a higher fraction of precipitating cloud particles to small cloud-ice particles in this region compared to in the westerlies regions. The average IWP has approximately the same relative fraction in continental convective regions as for the maritime region, albeit a little less, with the strong exception of MSPPS. MSPPS average IWP for the tropical continental region is nearly a factor five higher than its total

IWP spatial distribution comparison

S. Eliasson et al.

Title Page

Abstract

Introduction

Conclusions

References

Tables

Figures

◀

▶

◀

▶

Back

Close

Full Screen / Esc

Printer-friendly Version

Interactive Discussion



average. This could be as MSPPS best detects deep convection, and deep convection is generally more intense and more frequently occurring over land (Hong et al., 2005). The results of the regional comparison further confirm the general assumptions on the different satellite data set properties presented in Waliser et al. (2009). Problems associated with comparing data sets where there are large diurnal variations of IWP, such as over the maritime continent are assumed to be small in the this study. CloudSat, NOAA18 (for MSPPS) and Aqua (for MODIS) are platforms in the A-train, and their local overpass times at the equator are around 01:45 a.m. and 13:45 p.m. As ISCCP is based on geostationary satellites and PATMOS-x is based on composite data from several sun-synchronous satellites, they may deviate from the other data sets due to different diurnal sampling.

The models are in agreement with satellite data in terms absolute IWP in the oceanic subsidence regions, however on a relative scale they are not. All models except UKMO, have a relative IWP of between 27%–42%, whereas UKMO has a relative IWP value of 7%. The climate models are in greatest agreement with observed data in the Westerlies region. As modelled IWP should be lower than satellite retrieved IWP by definition, this probably indicates that the models tend to overestimate IWP in these regions. The exceptions are GISS and UKMO. GISS has very large IWP values and UKMO has a relative IWP value a factor three larger than its total average. In the convective regions all of the models have particularly low absolute and relative IWP values compared to the satellite data sets. This is especially pronounced in the tropical continental regions. UKMO stands out with very low IWP in these regions, merely around 30% of the total IWP. The low modelled IWP averages in this region are at least in part due to the low cloud-fraction, but in addition it may also indicate insufficient moist convection. It has previously been shown that climate models have strong limitations in modelling the diurnal cycle (Dai and Trenberth, 2004), of which may cause the models to underestimate the convection induced by surface heating. Also, the model regional results may reflect the better availability of surface and atmospheric data at mid-latitudes, which enables better parametrisations and tuning for the mid-latitudes. Whereas the tropics are

**IWP spatial
distribution
comparison**

S. Eliasson et al.

Title Page

Abstract

Introduction

Conclusions

References

Tables

Figures



Back

Close

Full Screen / Esc

Printer-friendly Version

Interactive Discussion



largely made up of oceans and monitored by a very sparse network of measurement sites, leading to poorer results.

As mentioned earlier, Waliser et al. (2009) found tropical, extra-tropical and global averages for all models and data sets. For example, by attaining a tropical average by latitude only, large areas with high IWP, such as trop_cont and warm_pool are averaged with large dry regions, such as ocean_sub along with large deserts (e.g. Sahara). Whereas, the average IWP of the extra-tropics is attained from regions with, in general, less extreme IWP differences. This regional comparison indicates that additional important information can be attained by comparing data sets and models on a regional basis, such as done here. Our results show that the IWP magnitude of the tropical “wet” regions is approximately a factor 2 higher than the extra-tropical “wet” regions for CloudSat. The GCMs show that IWP associated with the westerlies are generally twice as high as the total average, in accordance with Waliser et al. (2009). This survey showed additionally that modelled IWP in tropical continental regions is markedly lower than over tropical maritime convective regions. This may be predicted as ice clouds associated with convection over land, may have low cloud-ice fractions by comparison. Amongst the chosen subset of models, the spatial distribution of IWP is best modelled by ECHAM followed by CSIRO. UKMO is in largest disagreement with observations, in that it has much too low tropical IWP values and has quite high values in the westerlies. GISS has a very high IWP bias compared to all data sets, but is also in disagreement with the relative distribution of IWP.

4 Discussion and summary

The large discrepancies in modelled IWP distributions shown throughout this article reflect the difficulty in modelling this quantity. A major contributing factor to this is the lack of detailed cloud-ice measurements to constrain the models with. Although satellite data sets of IWP now span 25 years, their level of detail and accuracy on cloud ice are limited. The introduction of the CloudSat Profiling Radar is a leap forward for the

IWP spatial distribution comparison

S. Eliasson et al.

Title Page

Abstract

Introduction

Conclusions

References

Tables

Figures



Back

Close

Full Screen / Esc

Printer-friendly Version

Interactive Discussion



modelling community in addressing the problems in cloud-ice simulation. In contrast to the IWP data from passive sensors, CloudSat provides information on the vertical structure of clouds, which is essential information in modelling fields such as IWP.

In contrast to models, CloudSat IWP represents the total mass of ice, including graupel and snow, which are not included in model IWP. As discussed in detail in Waliser et al. (2009), the distinction between different ice categories is natural and simple from a model point of view, but hard or even impossible from a measurement point of view. The only reasonably well defined quantity to measure is total IWP, but to what extent satellite data sets represent this depends strongly on the technique used.

CloudSat was recently used as the main reference data set of IWP, in a study where the distribution of modelled IWC was tested in two prognostic GCMs in Waliser et al. (2009). It was shown that there are differences in vertical distribution of IWP between the models and CloudSat. However, CloudSat's temporal range is too short to assess climate models on longer time scales. For this, we must utilise data sets with long temporal ranges. The influence of inter-annual variations would otherwise lead to biased climatic statistics.

As seen in Sects. 3.1 and 3.2, the satellite data sets have very different magnitudes and distributions of IWP. ISCCP, PATMOS-x and MSPPS disagree considerably with CloudSat at high latitudes, and only MODIS was shown to be in reasonable agreement across all latitudes. As there was considerable nonconformity of IWP measurements at high latitudes, satellite-model comparisons were deemed dubious outside the tropics. On the other hand, the good agreement between satellite data sets in the tropics (30 S–30 N) enabled a comprehensive study of model performance here. We compared all satellite data sets to CloudSat in search for suitable data sets for model comparisons. PATMOS-x and MODIS are closest to CloudSat on a monthly mean basis, where they have biases in the tropics of approximately $31 \frac{\text{g}}{\text{m}^2}$ (41%) and $-27 \frac{\text{g}}{\text{m}^2}$ (-36%), respectively, compared to CloudSat. Despite having a larger bias, PATMOS-x is a better reference data set because it is in reasonable agreement with CloudSat and is much longer than MODIS.

**IWP spatial
distribution
comparison**

S. Eliasson et al.

Title Page

Abstract

Introduction

Conclusions

References

Tables

Figures



Back

Close

Full Screen / Esc

Printer-friendly Version

Interactive Discussion



IWP spatial distribution comparison

S. Eliasson et al.

Title Page

Abstract

Introduction

Conclusions

References

Tables

Figures

◀

▶

◀

▶

Back

Close

Full Screen / Esc

Printer-friendly Version

Interactive Discussion



As reflected by results presented here, climate models disagree on the magnitude and spatial distribution of IWP, confirming the results of Waliser et al. (2009). Generally, the models have much lower IWP values than indicated by satellite data sets. The disagreement is strongest in regions with persistent convection, where the amount of IWP is generally strongly underestimated by most models. Some models such as INM and CCSM have particularly low total averages of IWP, less than 20% of the observed IWP. The UKMO model has very low averages in the tropics, and high averages outside the tropics. The GISS model is the exception, it has much higher IWP values than observed by satellite, across all latitudes. In this, one must consider that only the cloud-ice part of the total IWP is represented by the models here and that the cloud-ice fraction may vary between 10–50% depending on the latitude and the model (Waliser et al., 2009). Despite negative biases of more than 60 g/m² (70%), ECHAM and CSIRO were the two models in best agreement with the “observed” data in terms of magnitude and spatial correlation. The remaining models (except GISS) have lower IWP values in the tropics and their spatial distribution is poorly correlated with the observed distribution.

To put the quantity “monthly mean IWP” into perspective, the distribution of IWP values during a single month was analysed in Sect. 3.3. It was shown that the mean month IWP is the mean of very different atmospheric states, and the distribution is highly non-Gaussian.

For the climate of IWP distributions to be modelled correctly, they must also capture the annual cycle. We compared the modelled spatial distribution of the annual cycle of monthly mean IWP to observations. This was done by studying fields of the coefficient of variation. For example, we expect a high monthly variability, in regions such as the Indian sub-continent and Northern Australia, and a low variability in regions such as near the equator over the Indonesian archipelago, as seen in observations (top panels in Fig. 7). Section 3.5 shows that most models differ from the “observed” data in terms of where and how strong their annual cycle of IWP is. This may indicate that important seasonal features such as the Indian monsoon may not be simulated satisfactorily. Additionally, a regional comparison study in Sect. 3.6 showed that the models (except

GISS) underestimate IWP magnitudes in convective regions in the tropics. Particularly in the continental convection regions, the models have consistently very low averages.

5 Conclusions

IWP data from CloudSat, although likely to be the best estimate of total IWP, are not a sufficient to judge the climatology of IWP. The CloudSat data record is too short to account for inter-annual variations. We have evaluated five IWP data sets by comparing them to CloudSat in their period of overlap, in terms of distribution and magnitude of monthly mean IWP. ISCCP, one of the longest data sets, has low IWP values by comparison and has particularly low values in the tropics. MSPPS has the lowest IWP values of the data sets. This data set, based on passive microwave measurements has very low values in regions outside the tropics, though it has strength in detecting deep convective clouds. MODIS and PATMOS-x behaved most like CloudSat, with MODIS being in better agreement. PATMOS-x has a temporal range of 25 years compared to MODIS approximately 10 years.

Although it is difficult to compare retrieved IWP to modelled IWP, by utilising long term data sets such as PATMOS-x, the climate model community has 25 years of data with which to constrain their IWP distributions. We compared the magnitude and distribution of modelled IWP of a subset of models from the IPCC AR4 to observed IWP distributions. Our results are consistent with John and Soden (2006) and Waliser et al. (2009) that there are large discrepancies between the climate models used in AR4. We showed that all models appear to have problems modelling the spatial distribution of IWP. This is especially true in tropical convective regions, where the models have relatively very low IWP averages compared to observations. Comparisons of statistical quantities associated with spatial distribution, regional IWP and the annual cycle of IWP, consistently show that ECHAM is the GCM from AR4 closest to satellite observations.

IWP spatial distribution comparison

S. Eliasson et al.

Title Page

Abstract

Introduction

Conclusions

References

Tables

Figures



Back

Close

Full Screen / Esc

Printer-friendly Version

Interactive Discussion



IWP spatial distribution comparison

S. Eliasson et al.

Title Page

Abstract

Introduction

Conclusions

References

Tables

Figures

◀

▶

◀

▶

Back

Close

Full Screen / Esc

Printer-friendly Version

Interactive Discussion



In future studies, we would like to enhance our understanding of the differences between the observational data sets. This should be done on a pixel level on coincidental data, rather than using monthly means. We believe that utilising the long satellite data sets of IWP is key to constraining model IWP distributions. Future satellite sensors that measure IWP more directly than current sensors, such as the one proposed in Buehler et al. (2007), would also be desirable.

Acknowledgements. We wish to thank Oliver Lemke for helping to acquiring the data used and for his technical assistance along the way. We thank David Parker for useful comments. We acknowledge the modelling groups, the Program for Climate Model Diagnosis and Intercomparison (PCMDI) and the WCRP's Working Group on Coupled Modelling (WGCM) for their roles in making available the WCRP CMIP3 multi-model data set. Support of this data set is provided by the Office of Science, US Department of Energy. We acknowledge the NASA CloudSat project for the CloudSat data. We acknowledge Andrew Heidinger for providing the PATMOS-x data. We acknowledge the NOAA National Climatic Data Center (NCDC) Satellite Data Services for providing the ISCCP data. We acknowledge NASA LAADS web for providing the MODIS data. We acknowledge Lisa Neclos for helping us with archived MSPPS data, and to all involved with the NOAA CLASS archive. Viju John was supported by the UK Joint DECC and DEFRA Integrated Climate Programme – DECC/Defra (GA01101). Salomon Eliasson is financed by the Swedish Research Council.

References

Ackerman, S. A., Strabala, K. I., Menzel, W. P., Frey, R. A., Moeller, C. C., and Gumley, L. E.: Discriminating clear-sky from clouds with modis, *J. Geophys. Res.*, 103, 32141–32157, 2008. 12193

Atkinson, N. C.: Calibration, monitoring and validation of AMSU-B. *Adv. Space. Res.*, 28(1), 117–126, 2001. 12193

Atlas, D., Matrosov, S. Y., Heymsfield, A. J., Chou, M.-D., and Wolff, D. B.: Radar and radiation properties of ice clouds, *J. Appl. Meteorol.*, 34, 2329–2345, 1995. 12200

Austin, R. T., Heymsfield, A. J., and Stephens, G. L.: Retrievals of ice cloud microphysical

IWP spatial distribution comparison

S. Eliasson et al.

Title Page

Abstract

Introduction

Conclusions

References

Tables

Figures

◀

▶

◀

▶

Back

Close

Full Screen / Esc

Printer-friendly Version

Interactive Discussion



parameters using the CloudSat millimeter-wave radar and temperature, *J. Geophys. Res.*, 114, D00A23, doi:10.1029/2008JD010049, 2009. 12191

Buehler, S. A., Jiménez, C., Evans, K. F., Eriksson, P., Rydberg, B., Heymsfield, A. J., Stubenrauch, C., Lohmann, U., Emde, C., John, V. O., Sreerexha, T. R., and Davis, C. P.: A concept for a satellite mission to measure cloud ice water path and ice particle size. *Q. J. Roy. Meteorol. Soc.*, 133(S2), 109–128, 2007. 12210

Dai, A. and Trenberth, K. E.: The diurnal cycle and its depiction in the community climate system model, *J. Climate*, 17, 930–951, 2004. 12205

Eriksson, P., Ekström, M., Rydberg, B., Wu, D. L., Austin, R. T., and Murtagh, D. P.: Comparison between early Odin-SMR, Aura MLS and CloudSat retrievals of cloud ice mass in the upper tropical troposphere, *Atmos. Chem. Phys.*, 8, 1937–1948, 2008, <http://www.atmos-chem-phys.net/8/1937/2008/>. 12187

Ferraro, R. R., Weng, F., Grody, N. C., Zhao, L., Meng, H., Kongoli, C., Pellegrino, P., Qiu, S., and Dean, C.: NOAA operational hydrological products derived from the advanced microwave sounding unit, *IEEE T. Geosci. Remote*, 43(5), 1036–1049, 2005. 12193

Heymsfield, A. J. and Iaquinta, J.: Cirrus crystal terminal velocities, *J. Atmos. Sci.*, 57, 916–938, 2000. 12188

Heymsfield, A. J., Protat, A., Austin, R., Bouniol, D., Hogan, R., Delanoë, J., Okamoto, H., Sato, K., van Zadelhoff, G.-J., Donovan, D., and Wang, Z.: Testing IWC retrieval methods using radar and ancillary measurements with in situ data, *J. Appl. Meteorol. Clim.*, 47(1), 135–163, 2008. 12188, 12191

Hong, G., Heygster, G., and Kunzi, K.: Intercomparison of deep convective cloud fractions from passive infrared and microwave radiance measurements, *IEEE Geosci. Remote Sens. Lett.*, 2, 18–24, 2005. 12205

Intergovernmental Panel on Climate Change: Fourth Assessment Report: Climate Change 2007: The AR4 Synthesis Report, Geneva: IPCC, 2007. 12188

John, V. O. and Soden, B. J.: Does convectively-detrained cloud ice enhance water vapor feedback?, *Geophys. Res. Lett.*, 33, L23701, doi:10.1029/2006GL027260, 2006. 12187, 12209

King, M. D., Tsay, S.-C., Platnick, S. E., Wang, M., and Liou, K.-N.: Cloud retrieval algorithms for modis: Optical thickness, effective particle radius, and thermodynamic phase, Technical report, MODIS Science Team, MODIS Algorithm Theoretical Basis Document No. ATBD-MOD-05, 1997. 12193

IWP spatial distribution comparison

S. Eliasson et al.

Title Page

Abstract

Introduction

Conclusions

References

Tables

Figures

◀

▶

◀

▶

Back

Close

Full Screen / Esc

Printer-friendly Version

Interactive Discussion



Mohapatra, G. N., Panda, U. S., and Mohanty, P. K.: Annual cycle of surface meteorological and solar energy parameters over orissa. *Indian J. Radio Space Phys.*, 36, 128–144, 2007. 12202

Ramanathan, V., Cess, R. D., Harrison, E. F., Minnis, P., Barkstrom, B. R., Ahmad, E., and Hartmann, D.: Cloud-radiative forcing and climate: Results from the earth radiation budget experiment, *Science*, 243, 57–63, 1989. 12187

Rossow, W. B. and Garder, L.: Selection of map grid for data analysis and archiving, *J. Clim. Appl. Meteor.*, 23, 1253–1257, 1984. 12192

Rossow, W. B. and Schiffer, R. A.: ISCCP cloud data products, *B. Amer. Meteorol. Soc.*, 72, 2–20, 1991. 12191, 12192

Stephens, G. L., Vane, D. G., Boain, R. J., Mace, G. G., Sassen, K., Wang, Z., Illingworth, A. J., O'Connor, E. J., Rossow, W. B., Durden, S. L., Miller, S. D., Austin, R. T., Benedetti, A., Mitrescu, C., and the CloudSat Science Team: The cloudsat mission and the A-train, *B. Amer. Meteorol. Soc.*, 83, 1771–1790, 2002. 12190, 12193

Storelvmo, T., Kristjánsson, J. E., and Lohmann, U.: Aerosol influence on mixed-phase clouds in cam-oslo, *J. Atmos. Sci.*, 65, 3214–3230, 2008. 12192

Waliser, D. E., Li, J.-L. F., Woods, C. P., Austin, R. T., Bacmeister, J., Chern, J., Genio, A. D., Jiang, J. H., Kuang, Z., Meng, H., Minnis, P., Platnick, S., Rossow, W. B., Stephens, G. L., Sun-Mack, S., Tao, W.-K., Tompkins, A. M., Vane, D. G., Walker, C., and Wu, D.: Cloud ice: A climate model challenge with signs and expectations of progress. *J. Geophys. Res.*, 114, D00A21, doi:10.1029/2008JD010015, 2009. 12188, 12190, 12191, 12194, 12196, 12197, 12198, 12203, 12205, 12206, 12207, 12208, 12209, 12218

Wu, D. L., Austin, R. T., Deng, M., Durden, S. L., Heymsfield, A. J., Jiang, J. H., Lambert, A., Li, J.-L., Livesey, N. J., McFarquhar, G. M., Pittman, J. V., Stephens, G. L., Tanelli, S., Vane, D. G., and Waliser, D. E.: Comparisons of global cloud ice from MLS, CloudSat, and correlative data sets, *J. Geophys. Res.*, 114, D00A24, doi:10.1029/2008JD009946, 2009. 12194

Table 1. IPCC Global Climate Models. This table provides an overview of the resolution and country of origin for the subset of IPCC AR4 models used in this study.

Short Name	Horizontal Resolution	Atm. Layers	Model Name	Institute
ECHAM	1.9 × 1.9°	19	ECHAM5/MPI-OM	Max Planck Institute for Meteorology (Germany)
CCSM	1.4 × 1.4°	26	Community Climate System Model, version 3.0 (CCSM3)	National Centre for Atmospheric Research (USA)
CSIRO	1.9 × 1.9°	18	CSIRO Mark 3.0, Climate System Model	Commonwealth Scientific and Industrial Research Organisation (Australia)
GISS	5 × 5°	15	GISS ModelE-R atmospheric, General Circulation Mode	NASA Goddard Institute for Space Studies (GISS) (USA)
INM	5 × 4°	21	INMCM3.0	Institute of Numerical Mathematics, Russian Academy of Science
UKMO	1.25 × 1.875°	38	Hadley Centre Global Environmental Model, version 1 (HadGEM1)	Hadley Centre for Climate Prediction and Research and UK Met office

IWP spatial distribution comparison

S. Eliasson et al.

Title Page

Abstract

Introduction

Conclusions

References

Tables

Figures

◀

▶

◀

▶

Back

Close

Full Screen / Esc

Printer-friendly Version

Interactive Discussion



IWP spatial distribution comparison

S. Eliasson et al.

Table 2. Satellite data sets. First part of the table contains the short name of the satellite data set used in this study, the satellite instrument, and the number of satellite channels in a radiance spectrum. Second part shows the type of product used for IWP and the temporal coverage for the data set. Only data from the Aqua satellite are used in the MODIS data set and only data from the NOAA 18 satellite are used in the MSPPS data set.

Short Name	Type	Platform(s)	Sensor	Spectrum	No. Ch.
ISCCP	VIS/IR	Geostationary: GOES, GMS, METEOSAT Polar: NOAA	Spectrometers	0.6, 11 μm	2
PATMOS-x	VIS/IR	NOAA-15,16,17,18	AVHRR	0.6–12 μm	5
MODIS	VIS/IR	Aqua	MODIS	0.6–14.2 μm	13
MSPPS	MV (passive)	NOAA-18	MHS	89–183 GHz	5
CloudSat	MV (active)	CloudSat	CPR	94GHz	1

Short Name	Data Product	Temporal Range
ISCCP	Month mean WP from different cloud classes on an equal area grid (ca. 250 × 250 km).	198 307–200 806
PATMOS-x	Month mean IWP product on equal area grid (ca. 50 × 50km).	198 201–200 804
MSPPS	IWP footprint product.	200 501–200 912
MODIS	Month mean IWP product on 1° grid	200 207–200 812
CloudSat	Radar Only IWP footprint product.	200 607–200 908

[Title Page](#)
[Abstract](#)
[Introduction](#)
[Conclusions](#)
[References](#)
[Tables](#)
[Figures](#)
[Back](#)
[Close](#)
[Full Screen / Esc](#)
[Printer-friendly Version](#)
[Interactive Discussion](#)


Table 3. Monthly mean IWP Statistics for selected satellite data sets and climate models. Statistics are provided for the total region (60 S–60 N) and the tropical region (30 S–30 N). The Satellite data comparison is from 2007, and all data sets are on a common spatial resolution of 5° with CloudSat chosen as the reference data set. Model statistics are based on the month averages derived from 100 years of data on a 5° grid. As model IWP can not be readily compared to satellite data, ECHAM has been arbitrarily chosen as the reference model for these statistics.

Data sets	Total					Tropics				
	Mean	Std	Bias	RMSD	<i>R</i>	Mean	Std	Bias	RMSD	<i>R</i>
CloudSat	77	90	0	0	1.00	75	104	0	0	1.00
ISCCP	33	28	-44	88	0.61	23	23	-52	101	0.79
PATMOS-x	109	83	32	71	0.73	105	97	31	72	0.80
MODIS-aqua	58	44	-19	67	0.75	48	47	-27	76	0.82
MSPPS-noaa18	12	18	-65	103	0.64	15	22	-60	108	0.74
AR4-ECHAM	34	22	0	0	1.00	24	18	0	0	1.00
AR4-CCSM	18	13	-15	20	0.88	12	9	-12	17	0.79
AR4-CSIRO	42	35	8	22	0.85	25	22	1	15	0.76
AR4-GISS	211	234	177	284	0.56	115	169	91	187	0.31
AR4-INM	11	6	-23	29	0.66	10	7	-15	21	0.65
AR4-UKMO	39	46	5	34	0.75	11	12	-13	22	0.39

IWP spatial distribution comparison

S. Eliasson et al.

Title Page

Abstract

Introduction

Conclusions

References

Tables

Figures

⏪

⏩

◀

▶

Back

Close

Full Screen / Esc

Printer-friendly Version

Interactive Discussion



Table 4. Area-weighted mean IWP [$\frac{\text{g}}{\text{m}^2}$] for selected regions. The regional fraction of IWP (in %) denoted IWP_{rel} , follows the regional mean in brackets and is given in relation to the mean IWP for the total region (60 S–60 N). All available data have been used to retrieve the mean values. The local equatorial passing times for CloudSat, MODIS and MSPPS in this study are around 13:45 and 01:45 as they are in the A-train. PATMOS-x is a composite data set from several sun-synchronous satellites and ISCCP is based on geostationary satellites.

Data set	ocean_sub	trop_cont	warm_pool	westerlies	total
CloudSat	4.7 (6)	161.3 (209)	175.8 (227)	106.8 (138)	77.3
ISCCP	2.2 (7)	41.8 (140)	45.9 (154)	57.0 (191)	29.8
PATMOS-x	16.0 (15)	183.3 (173)	197.4 (187)	164.1 (155)	105.7
MODIS-aqua	4.4 (8)	95.3 (163)	104.7 (179)	91.9 (157)	58.5
MSPPS-noaa18	0.5 (4)	59.9 (488)	31.4 (256)	4.8 (39)	12.3
AR4-CSIRO	7.1 (17)	26.0 (62)	52.1 (124)	98.1 (234)	41.9
AR4-ECHAM	9.0 (27)	39.9 (118)	44.0 (130)	61.9 (184)	33.7
AR4-GISS	50.6 (23)	192.1 (88)	152.4 (70)	447.9 (206)	217.7
AR4-INM	4.6 (42)	9.7 (90)	16.0 (148)	15.0 (138)	10.9
AR4-CCSM	4.9 (27)	14.9 (81)	22.9 (125)	36.5 (198)	18.4
AR4-UKMO	2.8 (7)	10.2 (26)	12.8 (32)	118.2 (300)	39.4

IWP spatial distribution comparison

S. Eliasson et al.

Title Page

Abstract

Introduction

Conclusions

References

Tables

Figures

◀

▶

◀

▶

Back

Close

Full Screen / Esc

Printer-friendly Version

Interactive Discussion



IWP spatial distribution comparison

S. Eliasson et al.

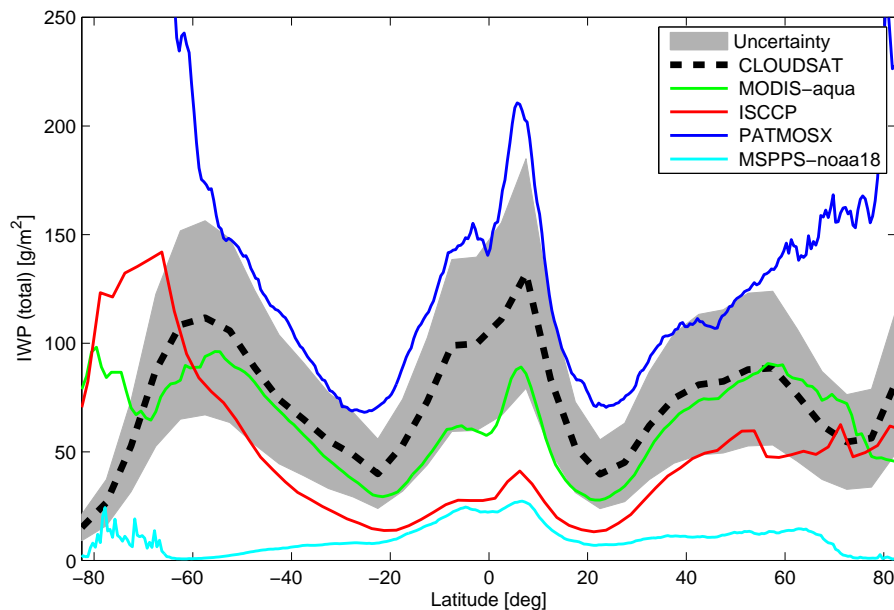


Fig. 1. Zonal averages of IWP from satellite data. The grey shaded area is the reference uncertainty interval, based on the uncertainty of CloudSat measurements (40%). The satellite data sets are averaged over the time period where the satellite data set temporal ranges overlap (July 2006 to April 2008).

[Title Page](#)[Abstract](#)[Introduction](#)[Conclusions](#)[References](#)[Tables](#)[Figures](#)[◀](#)[▶](#)[◀](#)[▶](#)[Back](#)[Close](#)[Full Screen / Esc](#)[Printer-friendly Version](#)[Interactive Discussion](#)

IWP spatial distribution comparison

S. Eliasson et al.

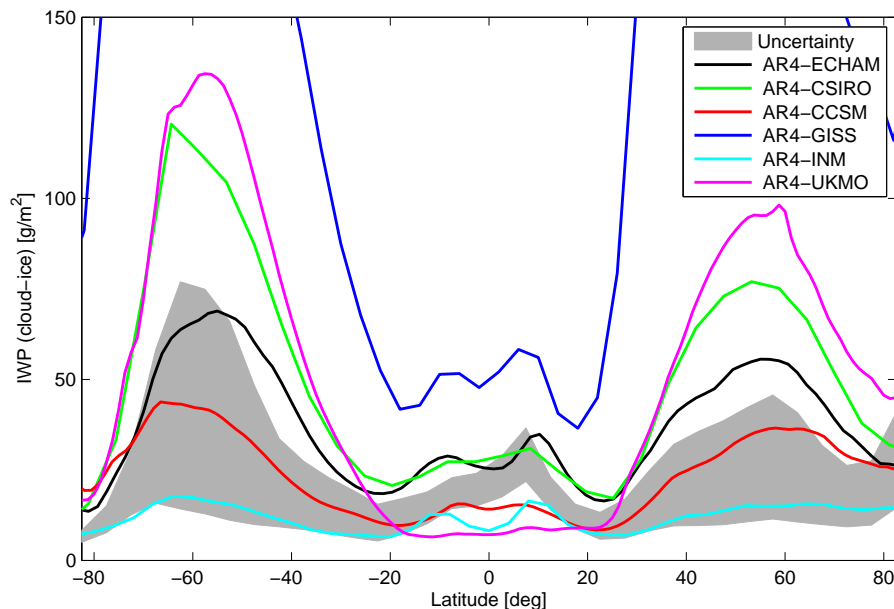


Fig. 2. Zonal averages of IWP for climate models from 100 years of monthly mean data. The upper and lower limits of the uncertainty range is based on a combination of CloudSat measurement uncertainties and the fraction of cloud-ice mass to total column mass of ice particles of two models presented in Waliser et al. (2009). See Sect. 3.1 for details. A factor 0.5 is applied to AR4-GISS in order for it to be visible in the domain of this figure.

Title Page

Abstract

Introduction

Conclusions

References

Tables

Figures

◀

▶

◀

▶

Back

Close

Full Screen / Esc

Printer-friendly Version

Interactive Discussion



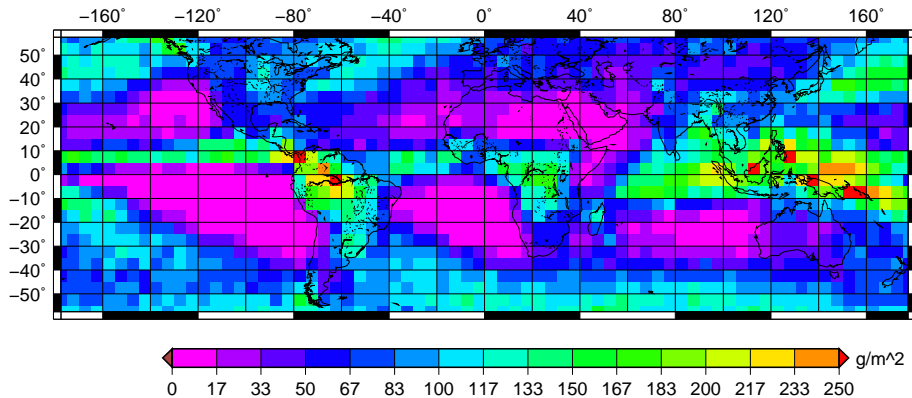


Fig. 3. Distribution of CloudSat IWP between 60 N and 60 S on a 5° grid, based on data from July 2006 to August 2009.

IWP spatial distribution comparison

S. Eliasson et al.

Title Page

Abstract Introduction

Conclusions References

Tables Figures

◀ ▶

◀ ▶

Back Close

Full Screen / Esc

Printer-friendly Version

Interactive Discussion



IWP spatial distribution comparison

S. Eliasson et al.

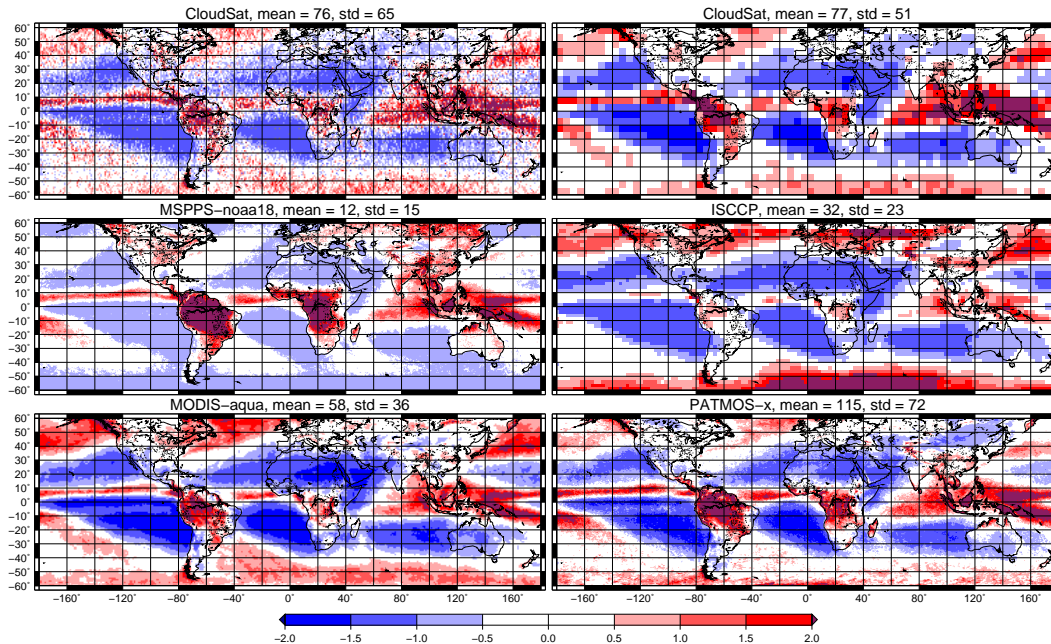


Fig. 4. Normalised satellite data of IWP, for their common temporal range (July 2006 to April 2008). IWP is normalised [unit-less] by subtracting the gridded area-weighted total mean and dividing by the total standard deviation. Figure titles contain the gridded mean and standard deviation (g/m^2) of each data set for latitudes 60 S–60 N. The absolute IWP averages can be re-acquired using these values. CloudSat is shown both on a 1° (left) and 5° (right) grid to illustrate how the dependence on the grid size influences the spatial statistics of CloudSat.

[Title Page](#)[Abstract](#)[Introduction](#)[Conclusions](#)[References](#)[Tables](#)[Figures](#)[◀](#)[▶](#)[◀](#)[▶](#)[Back](#)[Close](#)[Full Screen / Esc](#)[Printer-friendly Version](#)[Interactive Discussion](#)

IWP spatial
distribution
comparison

S. Eliasson et al.

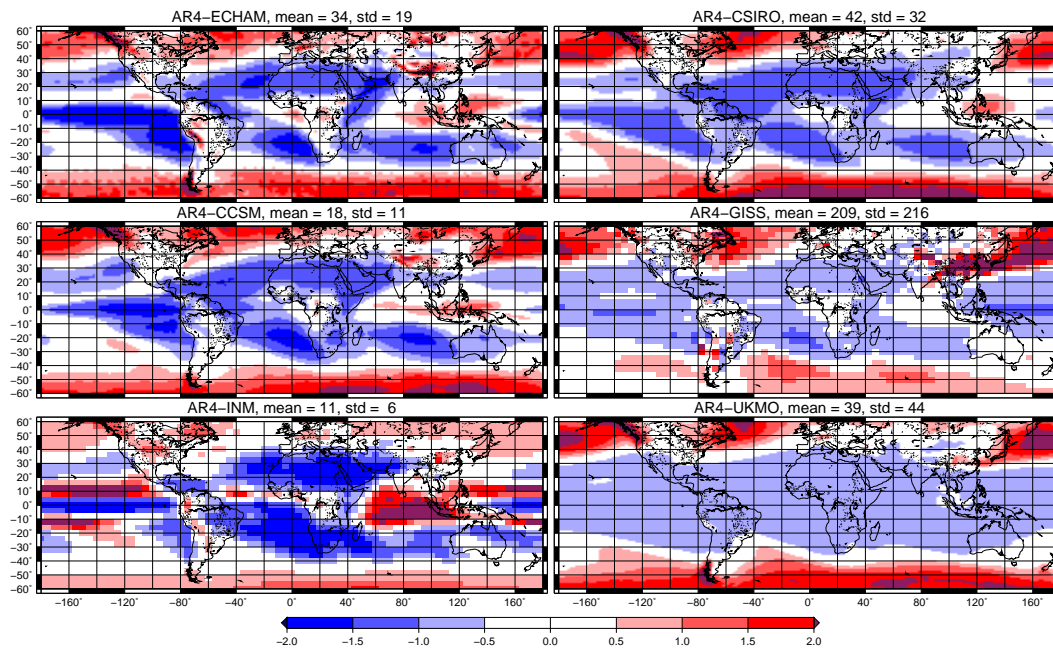


Fig. 5. Same as Fig. 4, except for model data, and all available monthly IWP data are used.

Title Page

Abstract

Introduction

Conclusions

References

Tables

Figures

◀

▶

◀

▶

Back

Close

Full Screen / Esc

Printer-friendly Version

Interactive Discussion



**IWP spatial
distribution
comparison**

S. Eliasson et al.

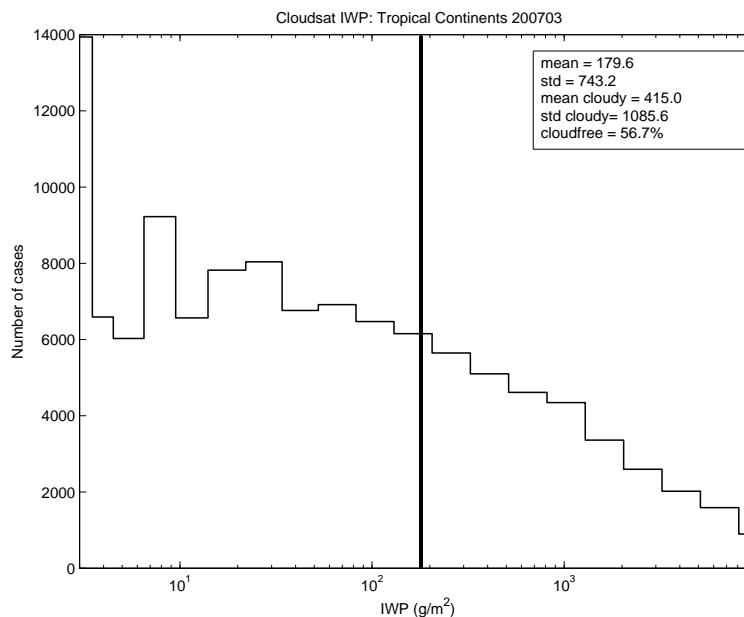


Fig. 6. Histogram of CloudSat IWP in a region of frequent strong convection. The region studied here is the combined regions of equatorial continental convection in South America and Africa and the month is March 2007. IWP is shown in intervals of $\log(\text{IWP})$. General IWP statistics from the region are provided in the text box. The vertical line intersecting the histogram represents mean IWP of the month.

Title Page

Abstract

Introduction

Conclusions

References

Tables

Figures

◀

▶

◀

▶

Back

Close

Full Screen / Esc

Printer-friendly Version

Interactive Discussion



IWP spatial
distribution
comparison

S. Eliasson et al.

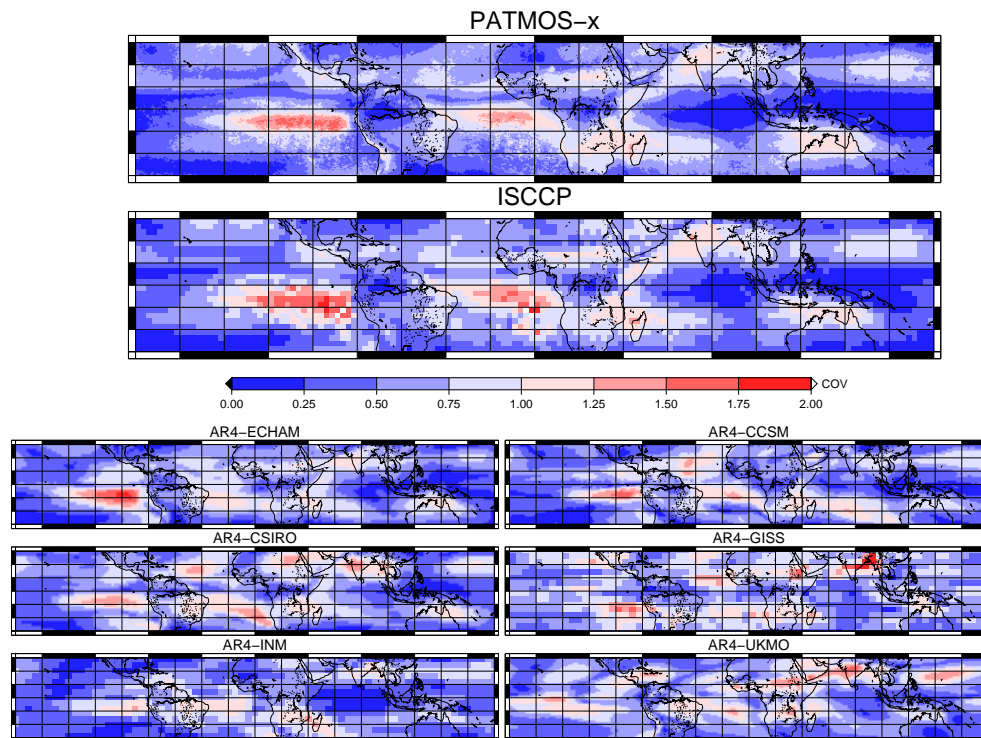


Fig. 7. Coefficient of variation, depicting the annual cycle of IWP. The top two panels are the data sets, PATMOS-x and ISCCP, both of which have sufficiently long temporal ranges to capture the inter-annual variability of IWP. The bottom six panels are the subset of models used in this survey.

[Title Page](#)[Abstract](#)[Introduction](#)[Conclusions](#)[References](#)[Tables](#)[Figures](#)[◀](#)[▶](#)[◀](#)[▶](#)[Back](#)[Close](#)[Full Screen / Esc](#)[Printer-friendly Version](#)[Interactive Discussion](#)

**IWP spatial
distribution
comparison**

S. Eliasson et al.

Title Page

Abstract

Introduction

Conclusions

References

Tables

Figures

◀

▶

◀

▶

Back

Close

Full Screen / Esc

Printer-friendly Version

Interactive Discussion

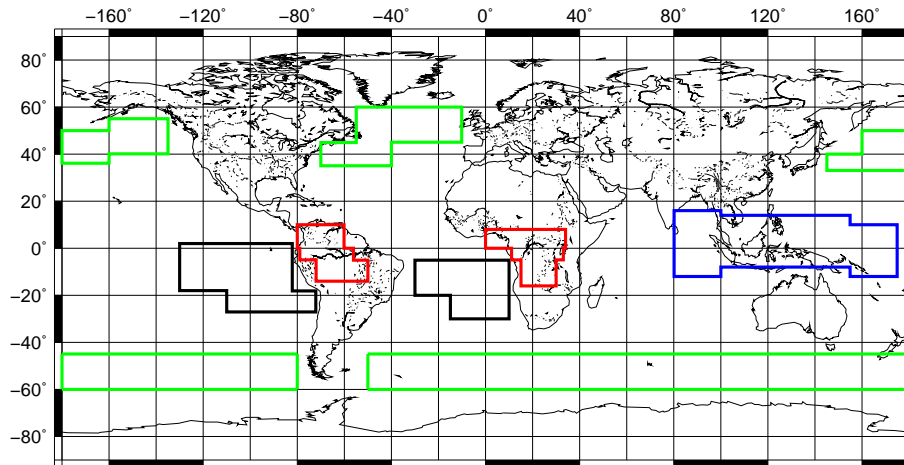


Fig. 8. Schematic of regions chosen for statistical comparison. Tropical Continental zones (red), Tropical maritime convective zone (blue), subsidence zones (black) and Westerlies (green).